Supporting Information

Reliable Manipulation of Gas Bubble Size on Superaerophilic Cones in Aqueous Media

Xiuzhan Xue, Ruixiao Wang, Linwen Lan, Jingming Wang, Zhongxin Xue, and Lei Jiang*

Ms. X. Xue, Mr. L. Lan, Ms. R. Wang, Dr. J. Wang, Prof. L. Jiang

Key Laboratory of Bio-Inspired Smart Interfacial Science and Technology of Ministry of Education, School of Chemistry, Beihang University, Beijing 100191, P. R. China.

E-mail: wangjm@buaa.edu.cn

Prof. L. Jiang

Laboratory of Bio-inspired Smart Interface Science, Key Laboratory of Bio-inspired Materials and Interfacial Science, Technical Institute of Physics and Chemistry, Chinese Academy of Sciences, Beijing 100190, P. R. China.

Dr. Z. Xue

School of Chemistry and Materials Science, Ludong University, Yantai, 264025, P. R. China.

S1 The reasons why superhydrophobic SiO_2 nanoparticles were chosen to modify the SCCs

There are many superhydrophilicity and superoleophobicity materials in aqueous media. In our manuscript, we have chosen a simple method by dip coating the mixture of hydrophobic fumed silica nanoparticles and poly(methyl methacrylate) (PMMA)/alcohol solution on SCCs. SCCs did not need any pre-or post-treatment. The hydrophobic SiO_2 nanoparticles create both microscale and nanoscale roughness, and provide low surface energy. PMMA acts as the binder to adhesive SiO_2 nanoparticles together. This method requires no further surface modification and can be applied to a variety of substrates over large areas. Furthermore, the proximity of roughness and thickness values is smaller than the 100 nm threshold. It will not change the shapes of SCCs.

S2 The wettability of SCC interface

On the smooth silicon wafer with superhydrophobic SiO_2 nanoparticle modification the water contact angle is 160.5 ± 2.5° and the gas contact angle approaches 0°. Only if the gas bubble radium (R_b) is larger than $2R_{scc}$ (R_{scc}, the curvature radius of the liquid–gas interface on SCCs), the gas bubble can be absorbed by the gas film on the SCC interface. That is to say, the gas bubble only can completely spread at the position where $R_b < 2R_{scc}$. If the $R_b < 2R_{scc}$, the gas bubble can sustain stability as a spherical crown shape on the SCC interface and then they are driven to the base side of SCCs under the gradient of Laplace pressure.

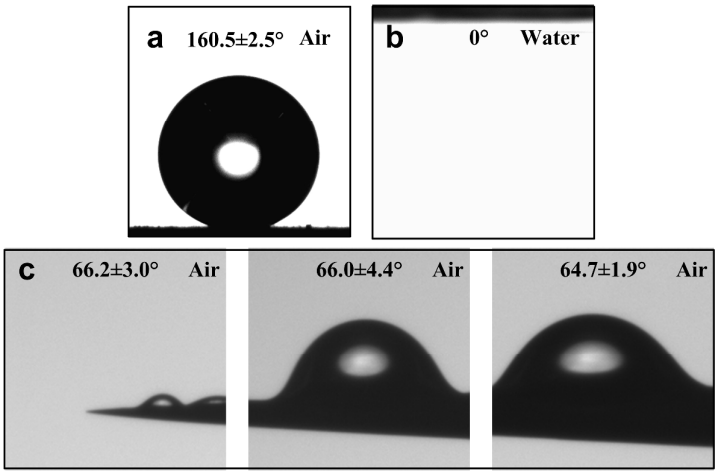

Figure S1. Wettability characterization of smooth silicon wafer with superhydrophobic SiO_2 nanoparticle modification and SCCs: (a) the water contact angle is 160.5 ± 2.5° and (b) the

gas contact angle approaches 0° on smooth silicon wafer with superhydrophobic SiO_2 nanoparticle modification; (c) The wettability of air bubbles with the diameter much larger than that of a SCC.

S3 The calculation of gas bubble volume

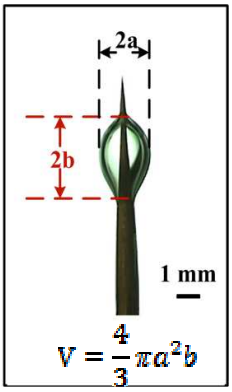

Figure S2. A gas bubble attached to the SCC interface can be regarded as an ellipsoid. Its volume can be calculated as: $V = 4/3\pi a^2 b$.

S4 The effect of SCC roughness on the gas bubble manipulation

We regulated the surface roughness by changed the quantity and diameters of SiO_2 nanoparticles. Surface height maps and sample surface profiles of SCCs with different roughness are illustrated in Figure S3. The roughness of the SCC without SiO_2 nanoparticle modification is 17.11 nm. If the SCCs modified with SiO_2 nanoparticles, the type of surface texturing/particle aggregation created by the assembly of the mixed nanoparticle multilayers: submicrometer-sized aggregated nanoparticles with a raspberry-like nanometer-sized outer surface. The RMS roughness of the SCCs modified with different quantity and diameters of SiO_2 nanoparticles is shown in **Table S1**. The RMS roughness on SCCs modified with [PMMA/(20 nm)SiO_2 (2.0)] chosen for gas bubble manipulation in our original manuscript is the largest (65.58 nm).

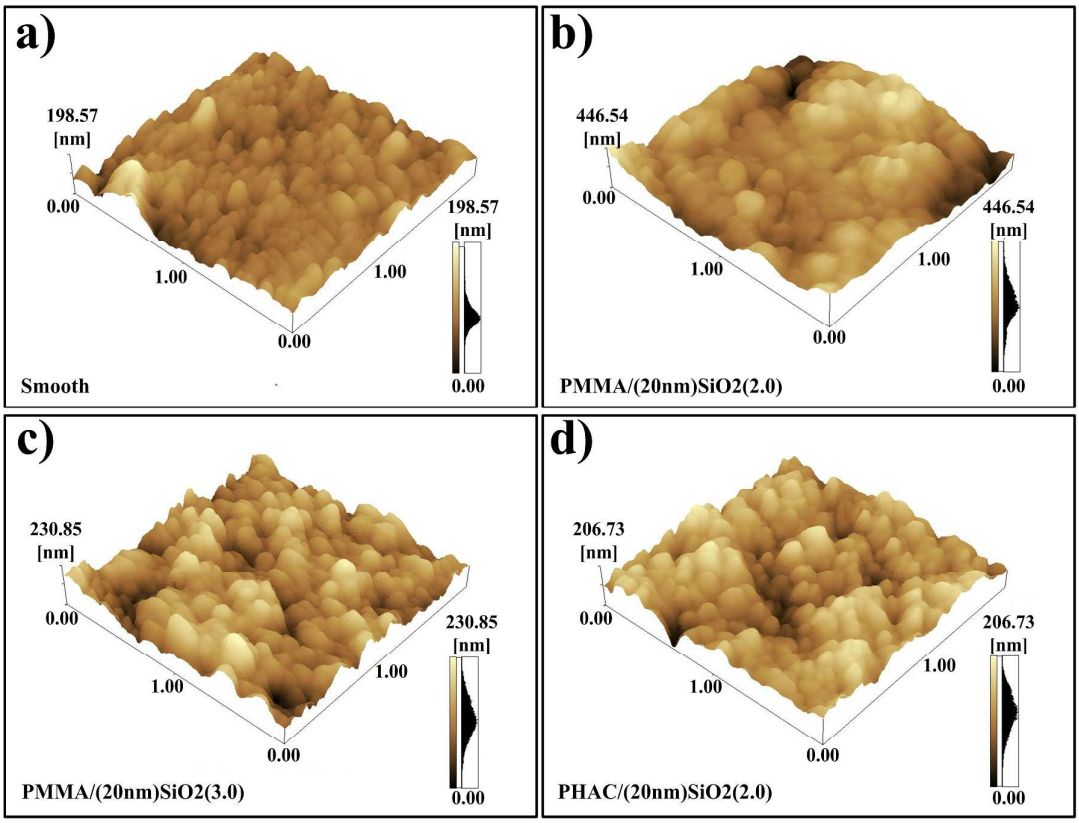

Figure S3. AFM images of surfaces of multilayers consisting of: a) FAS, b) [PMMA/(20 nm)SiO_2(2.0)]; c) [PMMA/(20 nm)SiO_2(3.0)]; d) [PHAC/(20 nm)SiO_2(1.0)].

When a gas bubble was injected to the copper cone that modified by fluoroalkylsilane (1H, 1H, 2H, 2H-heptadecafluorodecyl trimethoxy silane, FAS), the gas bubble just adhered to its interface as a sphere shape. With coalescing with more bubbles, the gas bubble grew. If its buoyance force exceeds the Laplace pressure and the axis-direction component of hysteresis resistance force impeding the movement of bubbles, the gas bubble move upwards along the CC. If the gas bubble is large enough, it finally left the CC (Figure S4).

The surfaces roughness significantly influences the contact state between the SCCs and the aqueous media. The contact state summarizes not only the thickness and distribution of the trapped gas layer, but also the axis-direction component of hysteresis resistance force impeding the movement of bubbles (F_H).

After investigating gas bubble behaviors on the SCCs with different roughness, we found that the SCC roughness can affect the movement of gas bubbles. With the decrease of SCC roughness, F_H increased and it is difficult for gas bubble to move. At the same L_b (the bubble's

balance position), the gas bubble volume at the SCC with small roughness is larger than that at SCC with large roughness. Correspondingly, the maximum volume V_{max} achieved at the SCC with small roughness is larger than that achieved at SCC with large roughness (Figure S5). The SiO_2 nanoparticles on the SCC modified with PMMA/(20 nm)SiO_2(3.0) are asymmetry. Thus, the gas bubble with small volumes can reach the middles part of the SCC. The maximum volume (V_{max}) achieved on the SCC (S-3) is smaller than that on SCCs (S-1 and S-2)

Table S1 The RMS roughness of the SCCs modified with FAS and different quantity and diameters of SiO_2 nanoparticles

No.	Nano Particle	Size/Diameter (nm)	Quantity ($\times10^{-2}$g/ml)	Polymer binder	RMS Roughness(nm)
N-1 Smooth	——	——	——	——	17.11
S-1 [PMMA/(20 nm)SiO_2(2.0)]	SiO_2(hydrophobic) Aerosil R202	20nm	2	PMMA	65.577
S-2 [PMMA/(20 nm)SiO_2(3.0)]	SiO_2(hydrophobic) Aerosil R202	20nm	3	PMMA	35.261
S-3 [PHAC/(20 nm)SiO_2(1.0)]	SiO_2(hydrophobic) Aerosil R202	20nm	1	PHAC	31.28

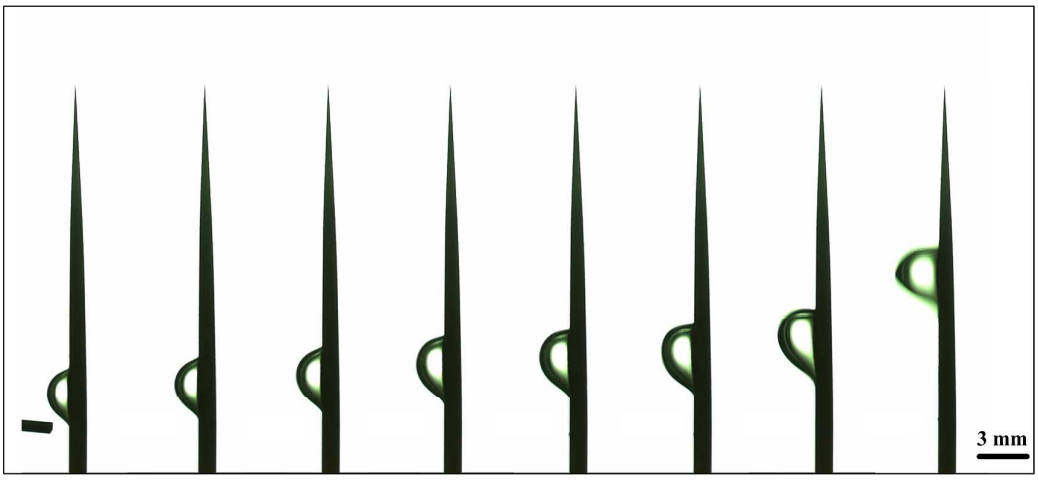

Figure S4. Dynamic balance of gas bubbles on FAS-CC interface.

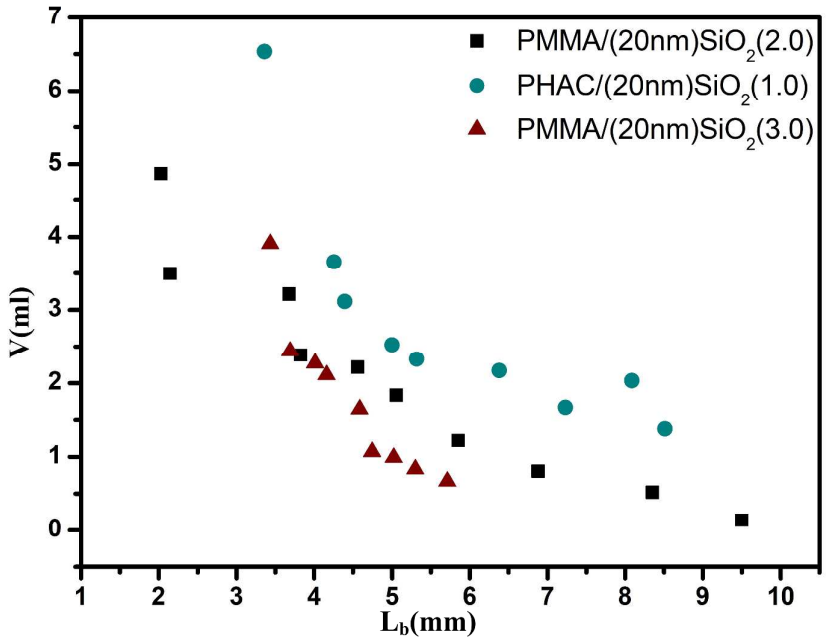

Figure S5. Variation of gas bubble volume at different balance position (L_b) on the SCCs with different roughness

S5 The calculation of the relation between L_b and V

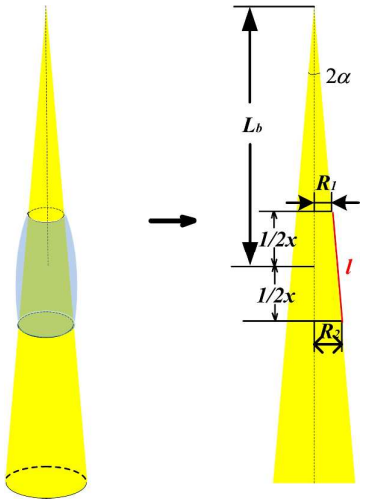

Figure S6. Schematic illustration of the relationship between the apex angle of cone (2α), the balance position (L_b), and the local radii at the two opposite sides of the gas bubble (R_1 and R_2).

The part of the SCC encapsulated by the gas bubble can be considered as a truncated cone. R_2 is radius of base circle; R_1 is radius of top circle; x is height or distance between the centers of

the base and the top circles; *l* is apothem or distance between any two closest points on the base and the top circles; $L_b+1/2x$ is distance between the center of the base circle and the imaginary point that connects all apothems.

$$\because \tan\alpha = \frac{R_1}{L_b - \frac{1}{2}x} = \frac{R_2}{L_b + \frac{1}{2}x}$$

$$\therefore R_1\left(L_b + \frac{1}{2}x\right) = R_2\left(L_b - \frac{1}{2}x\right)$$

$$R_1L_b + \frac{1}{2}R_1x = R_1L_b + \frac{1}{2}R_1x$$

$$\frac{1}{2}x\left(R_1 + R_2\right) = \left(R_2 - R_1\right)L_b$$

$$\therefore x = \frac{2\left(R_2 - R_1\right)L_b}{\left(R_1 + R_2\right)}$$

$$l = \sqrt{\left(L_b + \frac{1}{2}x\right)^2 + R_2^2} - \sqrt{\left(L_b - \frac{1}{2}x\right)^2 + R_1^2}$$

$$= \sqrt{\left[L_b + \frac{\left(R_2 - R_1\right)L_b}{R_1 + R_2}\right]^2 + R_2^2} - \sqrt{\left[L_b - \frac{\left(R_2 - R_1\right)L_B}{R_1 + R_2}\right]^2 + R_1^2}$$

$$= \sqrt{L_b^2\left(\frac{R_1 + R_2 + R_2 - R_1}{R_1 + R_2}\right)^2 + R_2^2} - \sqrt{L_b^2\left(\frac{R_1 + R_2 - R_2 + R_1}{R_1 + R_2}\right)^2 + R_1^2}$$

$$= \sqrt{L_b^2\left(\frac{2R_2}{R_1 + R_2}\right)^2 + R_2^2} - \sqrt{L_b^2\left(\frac{2R_1}{R_1 + R_2}\right)^2 + R_1^2}$$

$$= R_2\sqrt{\frac{4L_b^2}{\left(R_1 + R_2\right)^2} + 1} - R_1\sqrt{\frac{4L_b^2}{\left(R_1 + R_2\right)^2} + 1}$$

$$= \left(R_2 - R_1\right)\sqrt{\frac{4L_b^2}{\left(R_1 + R_2\right)^2} + 1}$$

$$S = \pi l\left(R_1 + R_2\right)$$

$$F_L = 2\gamma\left(\frac{1}{R_1}-\frac{1}{R_2}\right)S\sin\alpha$$

$$= \frac{2\gamma\left(R_2-R_1\right)}{R_1R_2}\pi l\left(R_2+R_1\right)\sin\alpha$$

$$= \frac{2\gamma\left(R_2-R_1\right)}{R_1R_2}\pi\left(R_2-R_1\right)\sqrt{\frac{4L_b^{\,2}}{\left(R_1+R_2\right)^2}+1}\left(R_2+R_1\right)\sin\alpha$$

$$= \frac{2\pi\gamma\left(R_2-R_1\right)^2}{R_1R_2}\sin\alpha\sqrt{4L_b^{\,2}+\left(R_1+R_2\right)^2}$$

$$= \rho Vg\sin\beta-\pi\gamma(\cos\theta_r-\cos\theta_a)\cos\alpha\left(\frac{3V}{4\pi}\right)^{\frac{1}{3}}$$

$$= F_B - F_H$$

$$\therefore \sqrt{4L_b^{\,2}+\left(R_1+R_2\right)^2} = \frac{-\rho Vg\sin\beta R_1R_2}{2\pi\gamma\sin\alpha\left(R_2-R_1\right)^2}$$

$$4L_b^{\,2} = \left(\frac{\rho Vg\sin\beta-\pi\gamma(\cos\theta_r-\cos\theta_a)\cos\alpha\left(\frac{3V}{4\pi}\right)^{\frac{1}{3}}}{2\pi\lambda\sin\alpha\left(R_2-R_1\right)^2}\right)^2 R_1^2R_2^2-\left(R_1+R_2\right)^2$$

$$L_b^{\,2} = \left[\frac{\rho Vg\sin\beta-\pi\gamma(\cos\theta_r-\cos\theta_a)\cos\alpha\left(\frac{3V}{4\pi}\right)^{\frac{1}{3}}}{4\pi\lambda\sin\alpha\left(R_2-R_1\right)^2}\right]^2 R_1^2R_2^2-\frac{1}{4}\left(R_1+R_2\right)^2$$

S6 The effect of salt on the gas bubble manipulation

The salt in the aqueous media will significantly change the surface tension. We have investigated the contribution of the salt in the bubble size in the NaCl solution with two concentrations (2.7 and 5.4 mol/L). According to the excess pressure formula on free gas bubbles, the bubble size in the NaCl solution is smaller than that in water resulting from their increased surface tension. Furthermore, the surfaces tension significantly influences the contact state between the SCCs and the aqueous media. The contact state summarizes not only the thickness and distribution of the trapped gas layer, but also F_H and F_L.

In order to investigate the contribution of the salt in the bubble manuscript, we used the SCC with apex angles of 3°, which are the most sensitive to the change of gas bubble volume, as shown in Figure S7. With increasing of surface tension, F_H increased a bit. It impeded the

movement of gas bubble. Thus, at high L_b (the position closed to the base side of the SCC), V in NaCl solution with concentration of 5.4 mol/L is larger than that in the water and in NaCl solution with concentration of 2.7 mol/L. With the decrease of L_b (the position closed to the top side of the SCC), V is similar in water and NaCl solution.

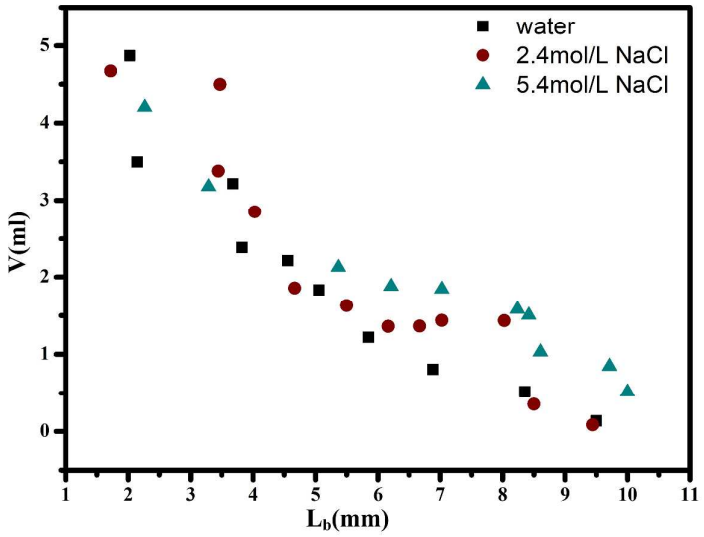

Figure S7. Variation of gas bubble volume at different balance position (L_b) in water and NaCl solutions.

S7 The relationship between L_b and outside pressure when the pressure were cycled multiple times in water and NaCl solution

When the pressure were cycled (i.e., decreasing and increasing) multiple times in water, L_b varies with increasing and decreasing of outside pressure; however, it is not same at the same outside pressure in each cycle (Figure S8). At first cycle, L_b decreased with the decrease of P_{out} due to the increase of the gas bubble volume. When the Pout decreased to -7.5 psi, L_b reached minimum value. Increasing the Pout, the volume of gas bubble decreased and the gas bubble started to move downwards only if the gas bubble is small enough, and L_b increased. When the first cycle finished, i.e., the outside pressure turned back to initial pressure (the atmospheric pressure), L_b reached the maximum value (L_{b1}) in the first cycle, and it cannot come back to the original position (L_{b0}). At second cycle, L_b changed from the starting point Lb1, the variation of L_b is similar as the first one. Furthermore, at the fifth cycle, the gas bubble cannot move

downwards with the increasing of Pout.

When the outside pressure decreased, water started to evaporate at water-air interfaces. With decreasing of the outside pressure, the volume of water vapor increased. Water vapor entered into not only the gas bubble but also the gas layer. When the Pout increased, water vapor in the gas bubble cannot completely condense to water. Thus, after the first cycle, the volume of gas bubble grew a bit larger. Furthermore, when the water vapor that entered into gas layer, the hysteresis resistance force increased to impede the movement of gas bubble. Correspondingly, after the first cycle, L_b cannot come back to the original position (L_{b0}). Similarly, if we repeated the decreasing and increasing Pout, the volume of gas bubble increased a bit, and F_H increased a lot. At the fifth cycle, the gas bubble cannot move downwards with the increasing of P_{out} and L_b did not changed.

In order to eliminate the effect of water vapor on gas bubble volumes, we investigated the dynamic balance cycles of single gas bubble on SCC interface in 5.4 mol/L NaCl solution. At the first cycle, L_b decreased with the decrease of P_{out} due to the increase of the gas bubble volume. When the P_{out} decreased to -6.0 psi, L_b reached the first local minimum value. Increasing the P_{out}, the volume of gas bubble decreased, however, the gas bubble didn't move downwards. When the first cycle finished, i.e., the outside pressure turned back to initial pressure (the atmospheric pressure), L_b still kept at the same position (L_{b1}). At the second cycle, L_b changed from the starting point L_{b1}. Lb decreased with the decreasing of Pout. After L_b dropped to the second local minimum value (L_{b2}), Lb increased with the increasing of Pout. Similarly, L_b cannot reach the original position of the second cycle ($L_{b2}<L_{b1}$). At the third and fourth cycles, the gas bubble moved downwards little with the increasing of P_{out}.

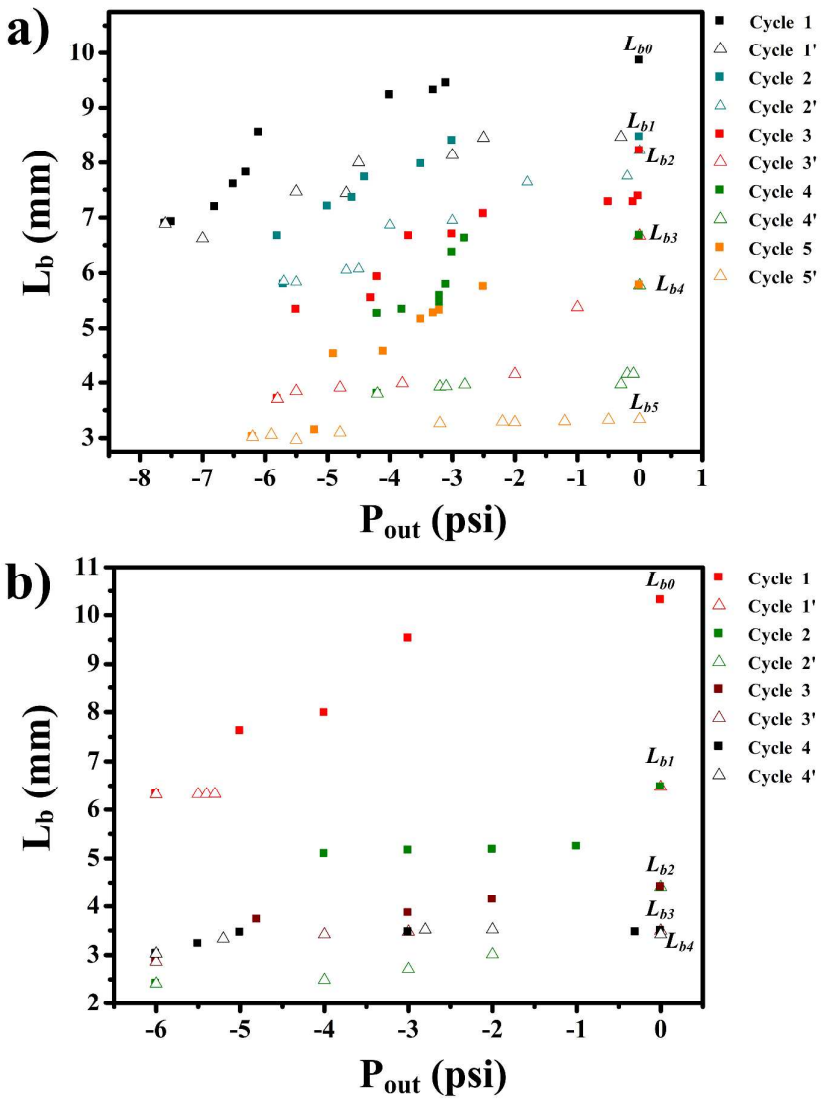

Figure S8. Dynamic balance cycles of single gas bubble on SCC interface in water and in NaCl solution with concentration of 5.4 mol/L. Cycle 1, 2, 3, 4 and 5: decreasing processes of P_{out}; Cycle 1', 2', 3', 4' and 5': increasing processes of P_{out}.

Video 1: Dynamic balance process of one gas bubble released at tip side of SCC.

Video 2: Dynamic balance process of one gas bubble released at base side of SCC.

Video 3: Dynamic balance process of one gas bubble merging with another gas bubble on SCC interface.

Video 4: Maximum volume of gas bubble held on the tip side of SCC.

Video 5: The change of gas bubble's position on SCC interface when decreasing system pressure.